Hypocycloid-shaped hollow-core photonic crystal fiber Part I: Arc curvature effect on confinement loss

B. Debord,[1] M. Alharbi,[1,2] T. Bradley,[1,2] C. Fourcade-Dutin,[1] Y.Y. Wang,[1] L. Vincetti,[3] F. Gérôme,[1] and F. Benabid[1,2,*]

[1]GPPMM group, Xlim Research Institute, UMR 7252 CNRS, Université de Limoges, Limoges, France
[2]Department of Physics, University of Bath, Claverton Down, BA2 7AY, UK
[3]Department of Engineering "Enzo Ferrari", University of Modena and Reggio Emilia, I-41125 Modena Italy
[*]f.benabid@xlim.fr

Abstract: We report on numerical and experimental studies showing the influence of arc curvature on the confinement loss in hypocycloid-core Kagome hollow-core photonic crystal fiber. The results prove that with such a design the optical performances are strongly driven by the contour negative curvature of the core-cladding interface. They show that the increase in arc curvature results in a strong decrease in both the confinement loss and the optical power overlap between the core mode and the silica core-surround, including a modal content approaching true single-mode guidance. Fibers with enhanced negative curvature were then fabricated with a record loss-level of 17 dB/km at 1064 nm.

OCIS codes: (060.5295) Photonic crystal fibers; (060.2280) Fiber design and fabrication.

References and links

1. P. Russell, "Photonic Crystal Fibers," Science **299**(5605), 358–362 (2003).
2. R. F. Cregan, B. J. Mangan, J. C. Knight, T. A. Birks, P. S. J. Russell, P. J. Roberts, and D. C. Allan, "Single-Mode Photonic Band Gap Guidance of Light in Air," Science **285**(5433), 1537–1539 (1999).
3. F. Benabid and J. P. Roberts, "Linear and nonlinear optical properties of hollow core photonic crystal fiber," J. Mod. Opt. **58**(2), 87–124 (2011).
4. P. J. Roberts, F. Couny, H. Sabert, B. J. Mangan, D. P. Williams, L. Farr, M. W. Mason, A. Tomlinson, T. A. Birks, J. C. Knight, and P. St. J. Russell, "Ultimate low loss of hollow-core photonic crystal fibres," Opt. Express **13**(1), 236–244 (2005).
5. F. Couny, F. Benabid, P. J. Roberts, P. S. Light, and M. G. Raymer, "Generation and Photonic Guidance of Multi-Octave Optical-Frequency Combs," Science **318**(5853), 1118–1121 (2007).
6. F. Benabid, J. C. Knight, G. Antonopoulos, and P. S. J. Russell, "Stimulated Raman Scattering in Hydrogen-Filled Hollow-Core Photonic Crystal Fiber," Science **298**(5592), 399–402 (2002).
7. A. Argyros, S. G. Leon-Saval, J. Pla, and A. Docherty, "Antiresonant reflection and inhibited coupling in hollow-core square lattice optical fibres," Opt. Express **16**(8), 5642–5648 (2008).
8. F. Couny, P. J. Roberts, T. A. Birks, and F. Benabid, "Square-lattice large-pitch hollow-core photonic crystal fiber," Opt. Express **16**(25), 20626–20636 (2008).
9. T. Grujic, B. T. Kuhlmey, A. Argyros, S. Coen, and C. M. de Sterke, "Solid-core fiber with ultra-wide bandwidth transmission window due to inhibited coupling," Opt. Express **18**(25), 25556–25566 (2010).
10. A. Argyros and J. Pla, "Hollow-core polymer fibres with a kagome lattice: potential for transmission in the infrared," Opt. Express **15**(12), 7713–7719 (2007).
11. Y. Y. Wang, F. Couny, P. J. Roberts, and F. Benabid, "Low Loss Broadband Transmission In Optimized Core-shape Kagome Hollow-core PCF," in Conference on Lasers and Electro-Optics (Optical Society of America, 2010), CPDB4.
12. Y. Y. Wang, N. V. Wheeler, F. Couny, P. J. Roberts, and F. Benabid, "Low loss broadband transmission in hypocycloid-core Kagome hollow-core photonic crystal fiber," Opt. Lett. **36**(5), 669–671 (2011).
13. T. D. Bradley, Y. Wang, M. Alharbi, B. Debord, C. Fourcade-Dutin, B. Beaudou, F. Gerome, and F. Benabid, "Optical Properties of Low Loss (70dB/km) Hypocycloid-Core Kagome Hollow Core Photonic Crystal Fiber for Rb and Cs Based Optical Applications," J. Lightwave Technol. **31**(16), 3052–3055 (2013).
14. A. D. Pryamikov, A. S. Biriukov, A. F. Kosolapov, V. G. Plotnichenko, S. L. Semjonov, and E. M. Dianov, "Demonstration of a waveguide regime for a silica hollow--core microstructured optical fiber with a negative curvature of the core boundary in the spectral region > 3.5 μm," Opt. Express **19**(2), 1441–1448 (2011).

#197514 - $15.00 USD Received 12 Sep 2013; revised 2 Nov 2013; accepted 5 Nov 2013; published 13 Nov 2013

15. F. Yu, W. J. Wadsworth, and J. C. Knight, "Low loss silica hollow core fibers for 3-4 μm spectral region," Opt. Express **20**(10), 11153–11158 (2012).
16. Y. Y. Wang, X. Peng, M. Alharbi, C. F. Dutin, T. D. Bradley, F. Gérôme, M. Mielke, T. Booth, and F. Benabid, "Design and fabrication of hollow-core photonic crystal fibers for high-power ultrashort pulse transportation and pulse compression," Opt. Lett. **37**(15), 3111–3113 (2012).
17. A. V. V. Nampoothiri, A. M. Jones, C. Fourcade-Dutin, C. Mao, N. Dadashzadeh, B. Baumgart, Y. Y. Wang, M. Alharbi, T. Bradley, N. Campbell, F. Benabid, B. R. Washburn, K. L. Corwin, and W. Rudolph, "Hollow-core Optical Fiber Gas Lasers (HOFGLAS): a review [Invited]," Opt. Mater. Express **2**(7), 948–961 (2012).
18. B. Beaudou, F. Gerôme, Y. Y. Wang, M. Alharbi, T. D. Bradley, G. Humbert, J. L. Auguste, J. M. Blondy, and F. Benabid, "Millijoule laser pulse delivery for spark ignition through kagome hollow-core fiber," Opt. Lett. **37**(9), 1430–1432 (2012).
19. B. Debord, M. Alharbi, T. Bradley, C. Fourcade-Dutin, Y. Wang, L. Vincetti, F. Gérôme, and F. Benabid, "Cups curvature effect on confinement loss in hypocycloid-core Kagome HC-PCF," in CLEO: 2013 (Optical Society of America, 2013), CTu2K.4.
20. W. Belardi and J. C. Knight, "Effect of core boundary curvature on the confinement losses of hollow antiresonant fibers," Opt. Express **21**(19), 21912–21917 (2013).
21. S. Selleri, L. Vincetti, A. Cucinotta, and M. Zoboli, "Complex FEM modal solver of optical waveguides with PML boundary conditions," Opt. Quantum Electron. **33**(4/5), 359–371 (2001).
22. L. Vincetti, "Numerical analysis of plastic hollow core microstructured fiber for Terahertz applications," Opt. Fiber Technol. **15**(4), 398–401 (2009).
23. L. Vincetti and V. Setti, "Confinement Loss in Kagome and Tube Lattice Fibers: Comparison and Analysis," J. Lightwave Technol. **30**(10), 1470–1474 (2012).
24. L. Vincetti and V. Setti, "Extra loss due to Fano resonances in inhibited coupling fibers based on a lattice of tubes," Opt. Express **20**(13), 14350–14361 (2012).
25. E. A. J. Marcatili and R. A. Schmeltzer, "Hollow Metallic and Dielectric Wave-guides for Long Distance Optical Transmission and Lasers," Bell Syst. Tech. J. **43**(4), 1783–1809 (1964).
26. L. Vincetti and V. Setti, "Waveguiding mechanism in tube lattice fibers," Opt. Express **18**(22), 23133–23146 (2010).
27. NKTphotonics, *http://www.nktphotonics.com/*.

1. Introduction

Hollow-core photonic crystal fiber (HC-PCF) consists of an optical-guiding central air-core surrounded by an arrangement of micro-scaled silica tubes running along its length [1]. Since its first experimental demonstration by Cregan *et al.* in 1999 [2] two main types of HC-PCF were established and their guidance mechanisms characterized [3]. The first HC-PCF family guides via photonic bandgap (PBG), and holds the potential for guiding light with attenuation several orders of magnitude lower than the fundamental limit of ~0.16 dB/km in conventional optical fibers, and which is set by the Rayleigh scattering in silica. Hitherto, however, the lowest loss obtained with this type of fiber is 1.2 dB/km [4]. This is set by the roughness of the air/glass interface and the presence of silica residing interface modes that couple with the core modes. This has not only limited the optical linear transmission performance but has also set several limits to the PBG guiding HC-PCF, such as poor optical power handling because of the subsequent strong overlap with the core silica-surround, and higher group velocity dispersion. Finally, another major limitation of this PBG guided HC-PCF is its limited transmission bandwidth (typically less than ~70 THz), which has hindered its use in applications where a large optical spectral band is required [3].

The second type of HC-PCF is distinguished by its broadband optical guidance and the relatively higher transmission loss-levels compared to the PBG guiding HC-PCF. This HC-PCF family guides via inhibited coupling (IC) between the cladding modes and the guided core modes. Unlike in PBG guiding HC-PCF, the cladding of the IC guiding HC-PCF doesn't exhibit any photonic bandgap but relies on a strong transverse mismatch between the continuum of cladding modes and those of the core, and the subsequent reduction of their field overlap integral. This guidance mechanism was proposed by Benabid and associates [5] to explain the salient features of Kagome-lattice HC-PCF, which was first reported in 2002 [6]. Subsequently, this guidance mechanism has been demonstrated in PCF with other cladding structures [7–9], including solid-core fiber [9] and different materials [7, 10]. Despite the effort in optimizing the cladding structure to further reduce the coupling between the cladding modes and those of the core, such as thinning the silica web of the HC-PCF

#197514 - $15.00 USD Received 12 Sep 2013; revised 2 Nov 2013; accepted 5 Nov 2013; published 13 Nov 2013

cladding and reducing the connecting nodes [5], the attenuation figures remained relatively high (>0.5 dB/m).

In 2010, we have proposed a new route in enhancing IC in Kagome HC-PCF and demonstrated a dramatic reduction of loss [11]. This consists of core-shaping the HC-PCF to a hypocycloid-like contour (i.e. with negative curvature) [11, 12] so as to minimize the spatial overlap between the high "azimuthal-like" number modes that reside in the silica core-surround and the zero-order Bessel-profiled core modes [13]. The second advantage of a negative curvature core-contour is that the connecting nodes of the silica are located further away from the mode field radius of the core compared to the circular core-surround. These connecting nodes are inherent to the fiber fabrication process, and support modes with a low azimuthal number, which subsequently strongly couple to the core modes. This seminal work [11,12] has proved to enhance the coupling inhibition even with single ring cladding [14], and to exhibit loss figures as low as 30 dB/km in the IR domain at 1.55 μm [15–17].

These new developments call for a further understanding on the relevant physical parameters behind the confinement loss. This is of interest in the fundamental physics underlying this novel optical guidance mechanism, and to assess IC guiding HC-PCF as a potential long-haul optical fiber. Furthermore, the use of this type of fiber in high-field physics is proven to be an excellent vehicle for ultra-short pulsed high power laser pulse delivery and compression [16], and for nanosecond laser pulse delivery with energy levels higher than 10 mJ [18].

Here and in a follow-up paper we explore respectively the effect of arc negative curvature of the hypocycloid core along with that of the cladding on the confinement loss in this Kagome HC-PCF. This effect was firstly reported by the present authors in [19], and then followed by [20]. In the present paper, we give a detailed account of what has been reported in [19] by reporting on experimental and numerical work showing the influence of the arc curvature of the hypocycloid-core on the loss figure of the fiber and on its modal properties. In section 2, we define the arc curvature and present the theoretical and experimental loss spectra for different arc curvatures. In section 3, we show the evolution with arc curvature of the optical power overlap between the core mode with the cladding silica struts, and of the core modal content. Finally, we present the fabrication of fiber exhibiting the largest arc curvature and a record loss level of 17 dB/km at 1064 nm.

2. Loss evolution with the arc curvature

Figure 1(a) shows a typical example of hypocycloid-like core HC-PCF with a Kagome lattice cladding. In the case considered here, the hypocycloid core contour results from 7 missing cells of a triangular arrangement of circular tubes. Consequently, the core contour is formed by two alternating arcs, which result in a small circle with radius R_{in} that is tangent with the 6 most inward arcs, and a larger circle with radius R_{out} which is tangent with the 6 most outward arcs. The curvature of the hypocycloid-like core is quantified through the parameter noted b (see Fig. 1(b)). The latter is defined as $b = d/r$, where d is the distance between the top of the arcs and the chord joining the nodes connecting the inward arc to its two neighboring ones and r is half the chord-length. With this definition, the "classical" Kagome fiber with a "quasi" circular core corresponds to $b = 0$, whilst $b = 1$ corresponds to a core contour with circular shaped arcs. For $0<b<1$ and $b>1$, the inward arcs have an elliptical shape whilst the outward ones are set to have a circular shape.

#197514 - $15.00 USD Received 12 Sep 2013; revised 2 Nov 2013; accepted 5 Nov 2013; published 13 Nov 2013

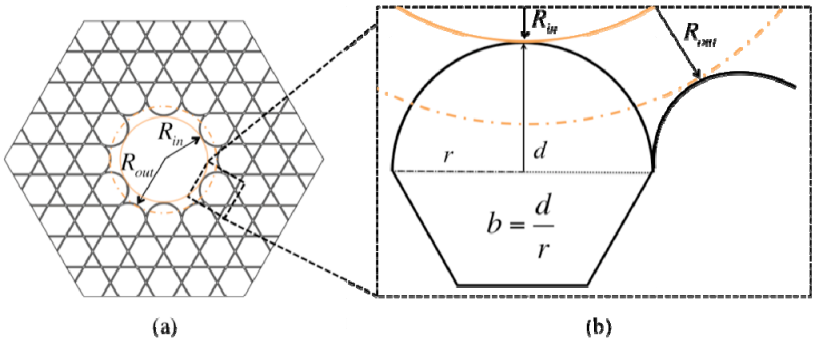

Fig. 1. (a) Structure of a hypocycloid-like core HC-PCF. (b) Definition of the parameters quantifying the curvature of the core arcs.

Figure 2(a) shows the calculated loss spectra of the HE_{11} core mode for a hypocycloid-like core Kagome-lattice HC-PCF with different arc curvatures. The numerical results have been obtained through the modal solver of the commercial software Comsol Multiphysics 3.5 based on the finite-element method, with an optimized anisotropic perfectly matched layer (PML) [21], and which was already successfully applied to the analysis of loss and dispersion properties of several IC HC-PCFs [22,23]. In the simulations, all the HC-PCFs have a 7-cell core defect and a Kagome-latticed cladding of 3 rings, and with strut thickness t equal to 350 nm. The HC-PCF structure has been studied for core arcs varying from b = 0 to b = 1.5. Furthermore, the core inner diameter (i.e. 2 × R_{in}) has been kept constant and equal to 60 μm throughout (see Fig. 2(b)). Consequently, this has an effect on the pitch Λ of the cladding which changes by $\Lambda\,\Lambda = [R_{in} + t(1-b/3)]/(\sqrt{3}-b/2)$

The calculated spectra clearly show the strong influence of the inward arc curvature on the loss confinement, and where the loss level drops from ~1000 dB/km in the case of a "quasi" circular core (i.e. b = 0) to lower than the 1 dB/km for hypocycloid core with b≥1. For a given structure, the loss spectrum exhibits a high loss spectral-region near 700 nm; corresponding to the resonance of the fundamental core-mode with the glass struts, and occurring at wavelengths λ_j given by the expression $\lambda_j = (1/j)2t\sqrt{n_{gl}^2 - 1}$, where j is an integer, n_{gl} is the refractive index of the glass forming the cladding structure and t is the thickness of the glass web which is assumed to be uniformly constant throughout the cladding structure [5]. Outside these spectral regions (i.e. the spectral ranges where the silica cladding structure is anti-resonant), the confinement loss exhibits an exponential-like decrease with the increase in the curvature parameter b. Figure 2(c) illustrates this trend for one wavelength in the first transmission band (λ_j = (1000 nm), and one wavelength at the second order transmission window (λ_j = 500 nm). It is noteworthy that all the confinement loss spectra exhibit relatively strong oscillations. These are attributed to resonant structural cladding features such as corners [5], and in some cases are Fano resonances [24]. These oscillations deserve further study which is beyond the current scope.

This trend of loss reduction with the increase in b has been experimentally confirmed with the fabrication of four Kagome-latticed fibers with different b. Figure 3(a) shows scanning electronic microscope (SEM) images of the fibers around the fiber core. Figure 3(b) shows the loss spectra in the fundamental band (i.e. for wavelengths longer than roughly twice the thickness of the silica struts [5]), obtained by a cutback measurement using a supercontinuum source, and fiber lengths were in the range of 50 to 70 m. The loss base-line level was found to be ~1300 dB/km for b = 0, 400 dB/km for b = 0.39, 200 dB/km for b = 0.68, and 40 dB/km for b = 0.75, which is in a qualitative agreement with the theoretical calculations. Care was taken in the fiber design and fabrication so as to have all the fibers with the same strut

#197514 - $15.00 USD Received 12 Sep 2013; revised 2 Nov 2013; accepted 5 Nov 2013; published 13 Nov 2013

thickness of 350 nm, core diameter of 60 µm and the pitch of 21 µm within a measured relative uncertainty of less than 10%. Figure 3(c) shows, for a given wavelength of 1500 nm, a comparison between the calculated confinement loss and the measured transmission loss when *b* is increased. The higher level in the measured loss relative to the numerical results is likely due to the cladding imperfections such as non-uniform strut thickness.

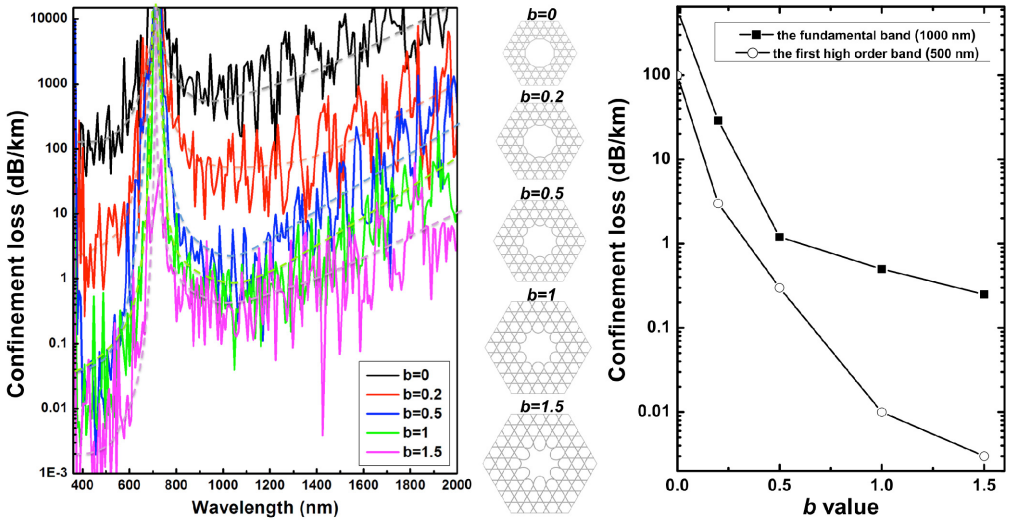

(a) (b) (c)

Fig. 2. (a) Kagome-latticed HC-PCF computed confinement loss evolution with the arc curvatures (*b* = 0, 0.2, 0.5, 1 and 1.5). The dashed lines are added for eye-guidance. (b) The fiber structure transverse profile for the different *b* values. (c) Evolution with *b* of the transmission loss figures for 1000 nm (joined solid squares) and for 500 nm (joined open circles) wavelengths.

#197514 - $15.00 USD Received 12 Sep 2013; revised 2 Nov 2013; accepted 5 Nov 2013; published 13 Nov 2013

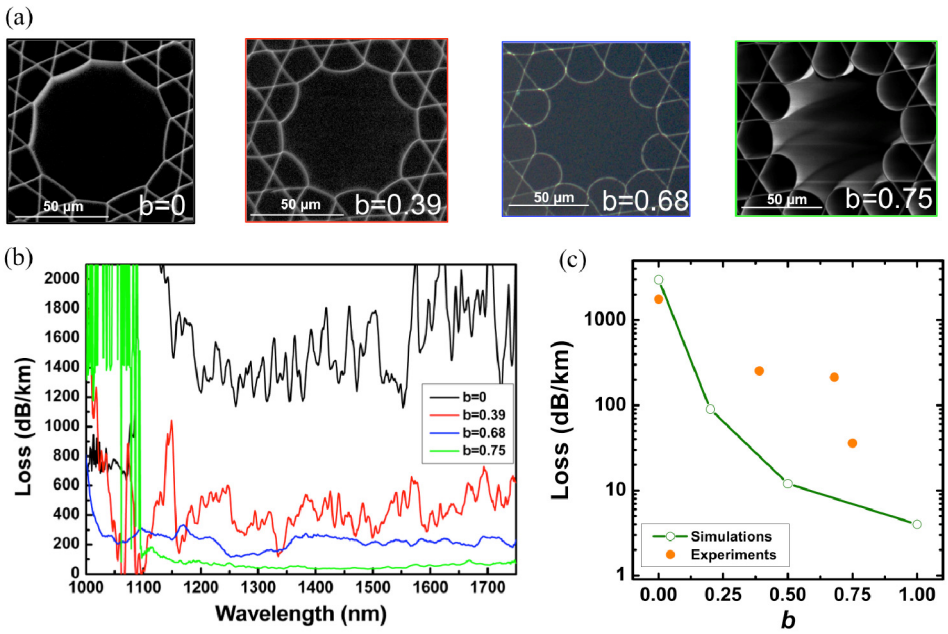

Fig. 3. SEM images (a) and measured loss spectra (b) of fabricated hypocycloid-core Kagome-latticed HC-PCFs with different *b*. (c) Experimental and theoretical evolution of the transmission loss with the *b* at 1500 nm.

3. Power overlap and modal content "cleansing" with increasing *b*

Figure 4 shows the evolution of the mode profile for the core fundamental mode (FM) HE_{11} with the increase of *b*. As above, the inner radius of the fiber R_{in} is still kept constant at 30 μm throughout all the simulations. We observe that the change of the curvature doesn't affect the mode profile (see Fig. 4(a)). More remarkably, the mode-field diameter MFD ($(1/e)^2$ diameter of the modal transverse profile) shows little change when *b* is altered from 0 to 1.5. This is illustrated by the radial profile of the mode along the two axes of the core-symmetry (i.e. along the axes of R_{in} and R_{out} respectively (see Fig. 1)), and where the MFD radii are shown in a vertical dashed line.

In order to gain further insight into the properties of the HE_{11} in this hypocycloid-core Kagome HC-PCF, it is useful to compare its MFD to that of a dielectric circular capillary whose properties such as dispersion and guided field profile takes simple and analytical forms [25]. For example in the case of a dielectric capillary with a bore radius R_{cap}, and a dielectric index n_g, the effective index and the MFD of the fundamental core-mode HE_{11} are given by $_{neff} = \sqrt{n_g^2 - (\lambda \times (2.405/2\pi R_{cap}))^2}$ and $MFD_{cap} = 0.7285(2R_{cap})$ respectively [25]. Here λ is the wavelength.

#197514 - $15.00 USD Received 12 Sep 2013; revised 2 Nov 2013; accepted 5 Nov 2013; published 13 Nov 2013

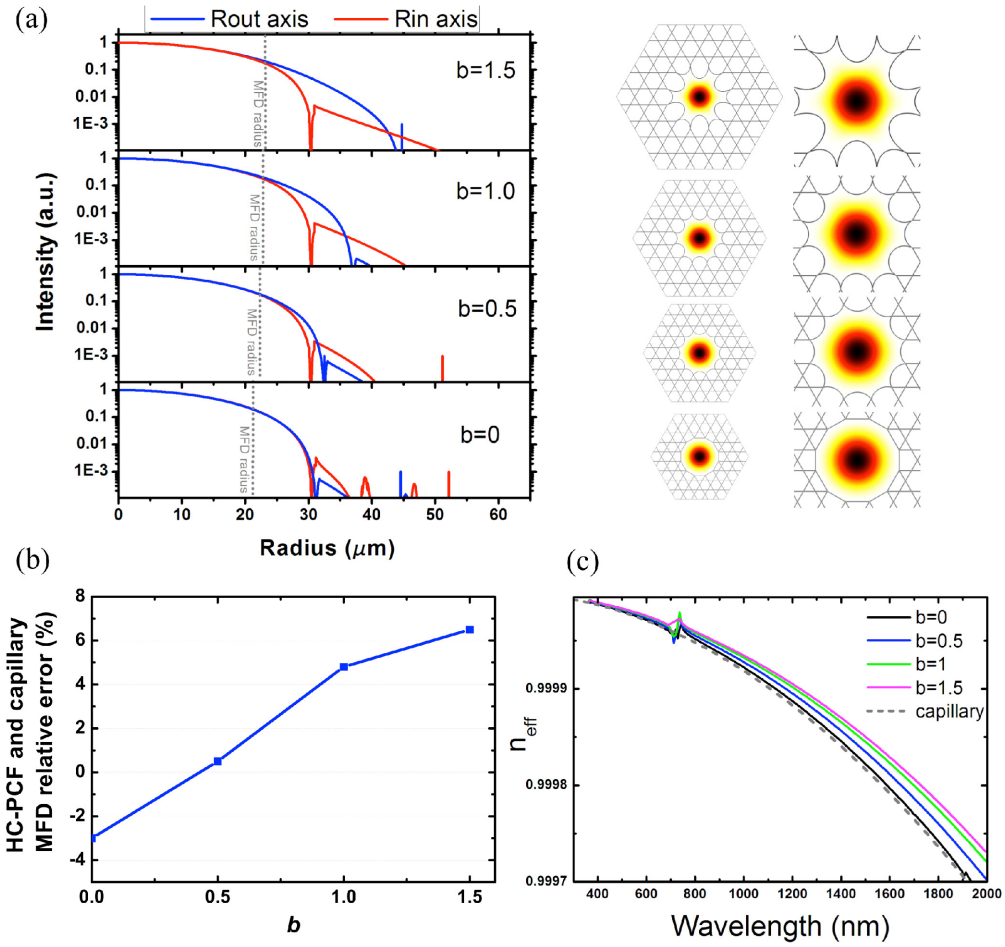

Fig. 4. (a) Evolution with b of HE_{11} mode profile at 1000 nm: Radial profile of the mode intensity along the two symmetry axes (lhs), and the 2D transverse intensity profile (rhs). (b) Evolution with b of the relative error in the MFD of hypocycloid-core Kagome HC-PCF when approximated to that of a capillary, at 1000 nm. (c) Effective index spectrum of a capillary with R_{cap} = 30 µm (grey dashed curve), and for a 30 µm inner radius hypocycloid-core Kagome HC-PCF with different b (solid curves).

Figure 4(b) shows the relative error, $(MFD_{cap} - MFD_{HCPCF}) / MFD_{cap}$, when the hypocycloid-core Kagome HC-PCF mode field-diameter, MFD_{HCPCF}, is approximated to that of a capillary, MFD_{cap}, with its radius $R_{cap} = R_{in}$. Here, the MFD_{HCPCF} is deduced from the numerically calculated effective area A_{eff} by. $MFD_{HCPCF} = 2\sqrt{A_{eff} / \pi}$.

The results indicate that within a maximum relative error of less than 7%, one could approximate the MFD of hypocycloid-core HC-PCF to that of a capillary with an effective radius equal to that of the inner radius of the hypocycloid. Similarly, the dispersion of the HE_{11} mode deviates little from that of the capillary when the curvature parameter b is increased from 0 to 1.5. Figure 4(c) shows the HE_{11} mode effective index spectra for different b along with that of a capillary with a bore radius of 30 µm. The dispersion traces show that the shorter the wavelength the closer the traces are. Furthermore, outside the resonance with the glass region, one could qualitatively approximate the effective index of hypocycloid-core Kagome HC-PCF fundamental mode to that of a dielectric capillary of bore radius equal to the inner radius of the hypocycloid-core.

#197514 - $15.00 USD Received 12 Sep 2013; revised 2 Nov 2013; accepted 5 Nov 2013; published 13 Nov 2013

A direct consequence of the above-mentioned properties of the hypocycloid-core Kagome HC-PCF fundamental core-mode is that its spatial optical power overlap (SPOPO) with the silica core-surround is reduced when the core shape is changed from a circular contour to a hypocycloid one. This is expected from a simple assessment of the geometrical overlap between the zero-order Bessel shaped HE_{11} mode and the core-contour at radius R_{in} [9,12]. A numerical corroboration is shown in Fig. 5, which gives, for a wavelength of 1 μm, the evolution with b of the fractional optical power residing in the cladding silica web for the core fundamental mode HE_{11} and the first four higher order modes (HOM) (represented only by one curve for better visibility as the curves for these four HOM are so closed to each other), which consist of the two polarizations of the HE_{21} mode, the TE_{01} and TM_{01} modes. The fractional power in silica η was deduced numerically using the following expression:

$$\eta = \frac{\iint_{S_{Si}} p_Z \, dS}{\iint_{S_\infty} p_Z \, dS},$$

where p_Z is the longitudinal component of the Poynting vector, while S_{si} and S_∞ indicate integration over the silica region and the whole cross section, respectively. The results show that the relative power ratio for the HE_{11} decreases by a factor of ~10 when b is increased from 0 to 0.5, and then decreases at a lower rate when b is increased from 0.5 to 2. The HOM fractional power in silica follows the same trend for the b in the range of 0-1.5. However for b>1.5 the overlap with silica strongly increases. This is due to the coupling between the HOM core modes and the inner arc hole modes (HM), that is the modes confined inside the holes of the large arcs surrounding the core. Figure 6(a) shows spectra of the effective index difference between the HOMs and the HM for b = 1.0, b = 1.5 and b = 1.9. The curves clearly show that increasing b from 1 to 1.9 reduces the index difference between the HOM and the HM, thus favoring coupling between them by virtue of phase matching. Indeed, as b increases, the hole size of the large arc increases, and thus the HM effective index increases and approaches that of the fiber core. This is also illustrated in the inset Fig. 6 which shows the intensity profile evolution of one of the HOM core modes (here HE_{21} mode) at 1 μm for b = 1.0, b = 1.5 and b = 1.9. For b = 1.9, the HE_{21} intensity profile differs strongly from those in the case of b = 1.0 and b = 1.5, and show a strong hybridization with the HM. This has already been experimentally observed in [5] and further investigated in [13,26]. As a result, since the HMs are much less confined than the HOM, the hybridization causes an increase in both the fraction power in silica and the confinement loss of HOM. The coupling between the HOM and HM is also indicative of the strong coupling inhibition between the core modes and the silica strut modes [5]. The decrease of the SPOPO between the fundamental core modes and the silica core-surround in the case of the hypocycloid-shaped core HC-PCF corroborates the qualitative picture reported in [11–13]. This also explains the high power handling demonstrated recently in [16].

#197514 - $15.00 USD Received 12 Sep 2013; revised 2 Nov 2013; accepted 5 Nov 2013; published 13 Nov 2013

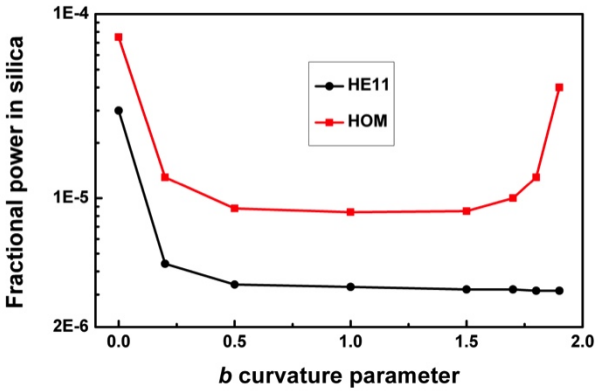

Fig. 5. The fractional optical power residing in the cladding silica, for a wavelength of 1 μm, for the core fundamental mode HE_{11} (black trace) and for the first four higher order modes: the two polarizations of the HE_{21} mode, TE_{01}, TM_{01} (red curve).

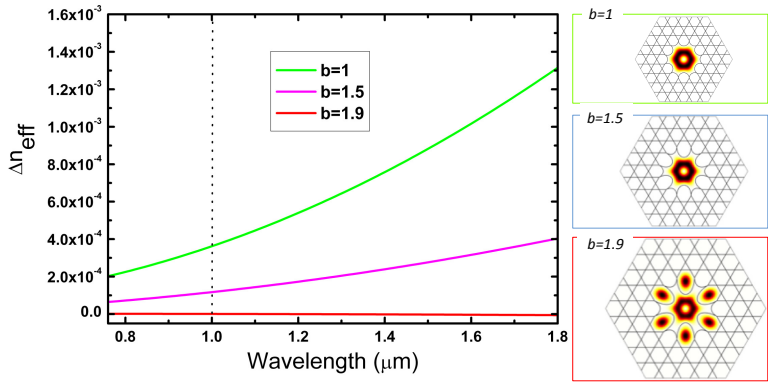

Fig. 6. Evolution with b of the effective index difference between the core first higher order modes (HOM), and the large arc mode (HMs) for b = 1.0, b = 1.5 and b = 1.9. In inset: intensity profile of the HE_{21} mode at 1 μm for the different b values.

It is noteworthy, that the decrease in the spatial overlap between the core guided modes and silica core-surround is not the only mechanism behind the confinement loss decrease by increasing b. Indeed, this can be observed in the decrease rate difference between the strong confinement loss (Fig. 2(c)), and that of the SPOPO when b is increased above 0.5 (Fig. 5). Furthermore, in addition to the SPOPO decrease between the core modes and those of the core silica-surround, the increase of b also results in a reduction of the overlap integral between the fiber core-modes and those of the silica core-surround via symmetry-mismatch (i.e. transverse phase-mismatch). Figure 7 summarizes the evolution around 1 μm wavelength of a representative silica core-surround mode when b is increased from 0 to 1.9 whilst keeping R_{in} to 30 μm. Figure 7(a) shows the intensity profile of a mode with closest effective index to that of HE_{11} mode for different b. For each b, the profile shows the expected silica-residing mode with a fast-oscillating transverse-phase [5]. The latter is quantified by an azimuthal-like number m which corresponds to the number of phase oscillations along the silica core-contour. Figure 7(b), which shows the evolution of m with b increase, clearly indicates that as b is increased, m is increased exponentially, and subsequently the overlap integral between the core mode and the silica core-surround is strongly decreased. The increase in m with b results from the increase in the perimeter of the hypocycloid contour as b is increased, as is illustrated by the red trace in Fig. 7(b). The net result of the azimuthal-like

#197514 - $15.00 USD Received 12 Sep 2013; revised 2 Nov 2013; accepted 5 Nov 2013; published 13 Nov 2013

number increase is an enhanced coupling inhibition between the fundamental core mode and the cladding modes, and subsequently a decrease in the experimentally observed confinement loss.

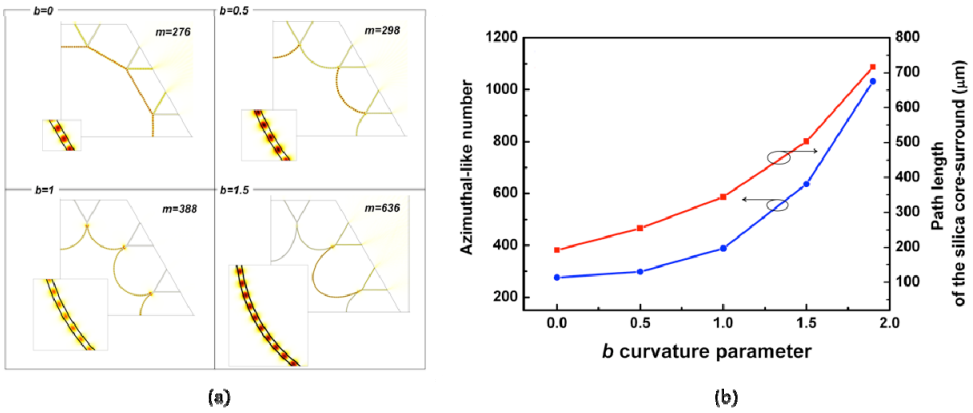

Fig. 7. (a) Profile of a representative silica core-surround mode for b = 0 (top left), b = 0.5 (top right), b = 1 (bottom left) and b = 1.5 (bottom right) at 1 μm. In inset: zoom-in of the cladding profile on a small section of the first inner arc. (b) Evolution of the azimuthal-like number m and the perimeter of the silica core-surround contour with b.

Finally, the increase of b carries a third merit as it involves the suppression of the higher order modes via propagation loss enhancement. Figure 8(a) shows the spectra loss for the four HOMs versus b at 1 μm wavelength (represented only by one curve for better visibility as the curves for these four HOM are so closed to each other). Unlike the HE_{11} loss, which keeps decreasing with b, the HOM confinement loss shows an increase for b larger than 0.5, which is due to the coupling with the HM as mentioned above. This explains the single modedness observed in [16]. Furthermore, the confinement loss "extinction-ratio" between the HE_{11} mode and the HOM increases from 0 dB for b<0.5 to 7 dB for b = 1, reaching the staggering figure of >100 dB for b = 1.9. These results clearly show that in order to have a near single-mode guidance, b should be much higher than 0.5. This is illustrated experimentally by inspecting the near-field and far field of the output of 1064 nm laser beam from 3m-long of two fabricated HC-PCFs with a b = 0.39 and b = 1 (see Fig. 8(b)).

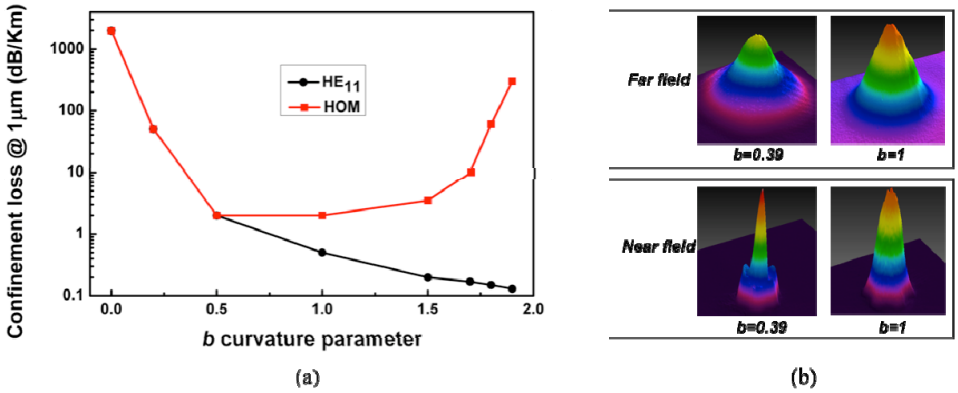

Fig. 8. (a) Calculated spectra loss at 1 μm for the fundamental core-mode HE_{11} and for the first four higher order modes. (b) Measured fundamental core-mode near field and far field at 1064 nm for 2 fabricated fibers with b = 0.39 and b = 1.

It is noteworthy that the HC-PCF with b = 1 was obtained with a silica strut thickness of 1400 nm instead of t = 350 nm, which is the thickness of all the fabricated fibers mentioned

#197514 - $15.00 USD Received 12 Sep 2013; revised 2 Nov 2013; accepted 5 Nov 2013; published 13 Nov 2013

above. This was dictated by the difficulties in drawing thin strut HC-PCF with enhanced negative curvature. Indeed, in the above, the highest achieved b parameter without altering the desired structure was limited to 0.75. Furthermore, we experimentally observed that with such thin struts, the higher-order transmission bands exhibit stronger transmission loss (>1 dB/m) than what is numerically predicted [2]. We believe that this is due to an enhanced capillary wave effect, and hence the fiber core-wall surface roughness during the fiber draw. Further investigations are required to assess the source of the higher loss in the short wavelength (< 700 nm in the case of our 350 nm thick strut HC-PCF), and the feasibility of enhanced negative curvature with the stack-and-draw process used here.

In order to achieve higher values than this experimental limit whilst keeping the same fabrication process, a new design of fiber has been explored based on thicker struts so as to mitigate the induced surface roughness mentioned above, and with the aim to optimize the loss for a wavelength around 1 µm. Numerical simulations show that ~1 dB/km loss-level could be obtained with thicker struts if b = 1 could be experimentally achieved (see Fig. 9(a)). The figure shows calculated loss spectra for three different t values, t = 350 nm, 800 nm and 1400 nm. Here the inner core radius has been set to be the same as the simulations above for the case of thinner struts (i.e. R_{in} = 30 µm). An attenuation level of ~1 dB/km at 1 µm was numerically predicted for the three fibers but in the fundamental band for t = 350 nm, in the second band for 800 nm and in the third for 1400 nm. It is noteworthy, that whilst thickening the struts would reduce the bandwidth of each transmission band, the fiber total bandwidth, unlike the PBG HC-PCF, remains unrestricted. Furthermore, this relative loss in bandwidth could be compensated by a more uniform strut thickness throughout the whole cladding structure, which narrows the high loss bands [5].

Figures 9(b) and 9(c) correspond to the loss spectra of two fabricated fibers with thicker struts with t = 800 nm and 1400 nm respectively. A maximum arc curvature of 0.9 is obtained for t = 800 nm. In contrast with thin-strut fibers, which exhibit strong attenuation in the higher-order transmission band, a loss figure as low as 80 dB/km was achieved in the first high-order band. This result was further corroborated with the t = 1400 nm fiber in which the wavelength of 1 µm lies in the second higher-order band. With this fiber, an arc curvature as high as b = 1 was successfully achieved, and a record loss fiber of 17 dB/km at 1064 nm was reached.

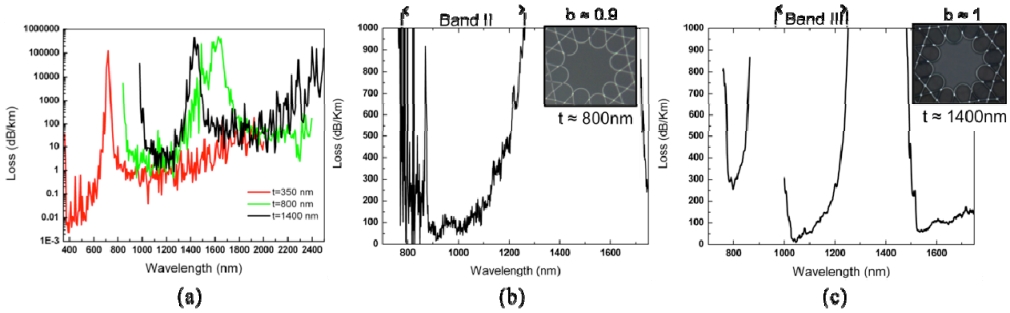

Fig. 9. (a) Computed loss of Kagome-latticed HC-PCFs with arcs curvature b = 1 for three strut thicknesses 350, 800 and 1400 nm; Measured loss of fabricated Kagome-latticed HC-PCFs with strut thickness (b) t = 800 nm and (c) t = 1400 nm. In inset, pictures of the core structures.

In order to put these results into perspective with the PBG guiding HC-PCF, Fig. 10 compares the loss spectra of two hypocycloid Kagome HC-PCF with the same strut thickness (here 1400 nm) and same b (here 1) but with slightly different drawing parameters, with four state-of-art commercially available PBG guiding HC-PCF [27]. Three of the fibers set are 7-cell PBG guiding HC-PCF whose transmission window is centered at ~800 nm, 1000 nm and 1550 nm respectively (light gray filled curves). The fourth fiber is today's record 19-cell PBG

#197514 - $15.00 USD Received 12 Sep 2013; revised 2 Nov 2013; accepted 5 Nov 2013; published 13 Nov 2013

guiding HC-PCF [4] (gray filled curve). The figure shows that whilst one single IC guiding Kagome HC-PCF guides a much wider spectral window than PBG HC-PCF, its loss figures are comparable. As a matter of fact, the loss is lower for Kagome HC-PCF in the region near 1 μm and 800 nm, indicating thus that IC guiding HC-PCF could be a good alternative to PBG HC-PCF for ultra-low loss guidance HC-PCF.

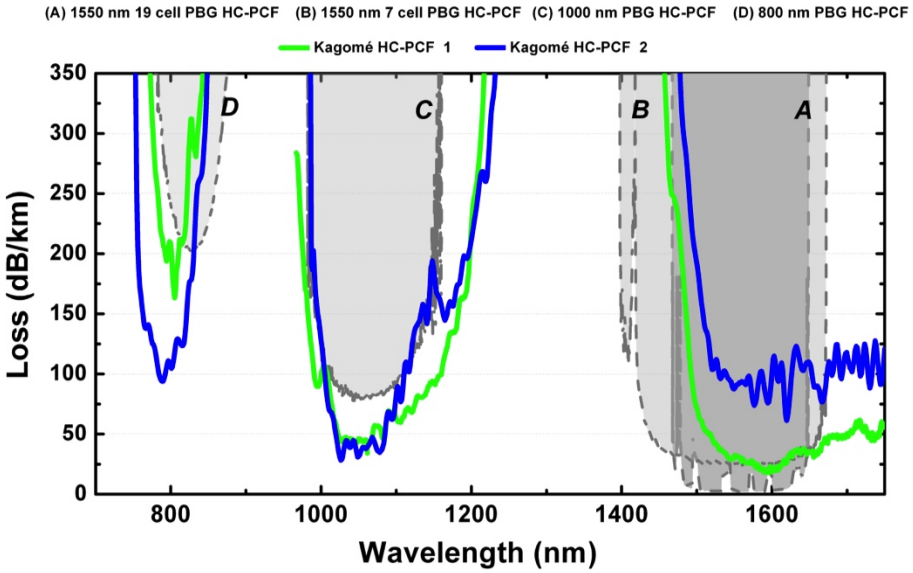

Fig. 10. Comparison of the loss spectra of the current lowest loss 19-cell BPG HC-PCF centered at 1550 nm (A), and three state-of-art 7-cell PBG HC-PCF centered at 800 nm (B), 1000 nm (C) and 1550 nm (D) with the two different hypocycloid-core Kagome HC-PCF with $b = 1$ (blue and green solid curves).

4. Conclusion

In conclusion, we reported a systematic numerical and experimental study on the effect of the hypocycloid-core Kagome HC-PCF negative curvature on the fiber transmission loss and its modal properties. The results showed that enhancing the core-surround curvature carries three merits: (i) several orders of magnitude decrease in the fundamental core-mode confinement loss, (ii) more than tenfold reduction in the fundamental core-mode power overlap with cladding silica, and (iii) nearing a truly single-mode guidance. The results show that the transmission loss of IC guiding HC-PCF can outperform the PBG guiding HC-PCF, as demonstrated with 17 dB/km transmission loss around 1 μm spectral range in $b = 1$ hypocycloid-core Kagome HC-PCF, whilst providing much larger bandwidth, a much higher optical power handling and a modal content approaching single-modedness.

Acknowledgments

The authors thank the PLATINOM platform for the help in the fiber fabrication. This research is funded by "Agence Nationale de la Recherche (ANR)" through grants PHOTOSYNTH and ∑_LIM Labex Chaire, Astrid UV-Factor and by "la région Limousin".

#197514 - $15.00 USD Received 12 Sep 2013; revised 2 Nov 2013; accepted 5 Nov 2013; published 13 Nov 2013